Study of the Evolution of Soot from Various Fuels

Shihong Yan,[†] Yi-Jin Jiang,[‡] Nathan D. Marsh,[†] Eric G. Eddings,[†] Adel F. Sarofim,[†] and Ronald J. Pugmire*[,†,‡]

Departments of Chemical Engineering and Chemistry, University of Utah, Salt Lake City, Utah 84112

Received October 15, 2004. Revised Manuscript Received April 29, 2005

JP-8, a surrogate fuel, and several model compounds were used to produce soot aerosols in a drop-tube furnace with optical access. The soluble organic fractions (SOF) of soot aerosols were studied with GC, GC−MS, and ^{13}C NMR. The residue of each aerosol sample was studied with Raman spectroscopy, ESR, and a recently developed technique used to determine the conductivity and extent of turbostratic structure formation in soot. The SOF values from different fuel sources exhibit variations in yield, and carbon aromaticity values, and the latter parameter correlates with the extent of turbostratic structure formation in the aerosol residues. Raman data of the soot residues indicate the presence of highly disordered graphitic structures, but the graphite factor measurements reveal differences among these disordered structures that are not apparent in the Raman data.

Introduction

Soot formation and release have become a major concern impacting both the environment and human health.[1] It is generally agreed that the formation of soot occurs as follows: (a) a complex process encompassing formation of radical precursors such as polycyclic aromatic hydrocarbons (PAH) through radical reactions of small molecules and/or fragments; (b) molecular growth; (c) nucleation; (d) coagulation; and (e) oxidation.[2] Numerous mechanisms have been proposed for the formation of precursors and growth of PAH.[3−5] Many of these research reports use simple gaseous fuels to study the formation of PAH and profiles of the soot volume fraction. Studies that employ transportation fuels, such as diesel and jet fuels, are more limited due to difficulty in vaporization, complexity in composition, and uncertainty in kinetic modeling. The study of surrogate fuels offers a means of simplifying these experiments since one is using a limited number of different molecular species with known kinetic parameters. For instance, Lindstedt and Maurice have recently reported a kinetic model for aviation fuels using a surrogate blend of 89 mol % *n*-decane and 11 mol % single ring aromatic compounds such as benzene and alkyl-substituted benzenes.[6] A previous study from this laboratory of a jet fuel surrogate formulation and associated modeling has demonstrated the capability of surrogate fuels to capture the main characteristics of real kerosene flames, such as the profiles of CO, CO_2, OH^-, and PAH.[7] Jet fuel surrogates have also been tested in pool fire scenarios in which the simulation of the steady state of a JP-8/Jet-A pool fire was demonstrated.[8] The present study is a continuation of efforts at the University of Utah in the use of surrogate fuels to simulate JP-8 droplets in a diffusion flame. The ability of a surrogate fuel to model the formation of soot in addition to the composition of the soot extract is compared during the combustion of both surrogate fuel and JP-8. Other model fuels are used in this study as well. The focus of these experiments is not directed specifically to the gas-phase chemistry but rather to the evolution route of soot from JP-8 and a few simple surrogate fuels.

Experimental Procedures

Fuels. The fuels tested in this study include JP-8, JP-8 surrogate (Hex-12), Decalin (mixture of trans and cis isomers), *n*-dodecane, and a mixture of 2,2,4-trimethylpentane (*i*-C_8) and toluene (*i*-C_8/toluene) at 80:20 vol/vol. Hex-12 is a surrogate fuel that closely matches the physical characteristics of JP-8. The compositions and properties of JP-8 and JP-8 surrogate (Hex-12) are listed in Table 1, and other physical properties of the fuels tested are given in Table 2. Detailed information on JP-8 and Hex-12 can be found in Eddings et al.[8]

Aerosol Production. Soot samples from JP-8, Hex-12, Decalin, and *i*-C_8/toluene were produced in a laminar diffusion flame in a drop-tube furnace with optical access. The scheme of the furnace and other operating parameters have been described in detail by Hanson.[9] The furnace wall temperature for these tests was 973 K. The flame was generated using air

* Corresponding author. Tel: (801) 581-7236; fax: (801) 585-6212; e-mail: Ronald.Pugmire@vpres.adm.utah.edu.
† Department of Chemical Engineering.
‡ Department of Chemistry.

(1) Harvey, R. G. *Polycyclic Aromatic Hydrocarbons: Chemistry & Carcinogenicity*; University Press: Cambridge, 1991.
(2) Richter, H.; Howard, J. B. *Prog. Energy Combust. Sci.* **2000**, *26*, 565.
(3) Bockhorn, H.; Fetting, F.; Wenz, H. W. *Ber. Bunsen-Ges. Phys. Chem.* **1983**, *87*, 1067.
(4) Frenklach, M.; Clary, D. W.; Gardiner, W. C. J.; Stein, S. E. *Proc. Combust. Inst.* **1984**, *20*, 887.
(5) D'Anna, A.; Violo, A. *Proc. Combust. Inst.* **1998**, *27*, 425.
(6) Lindstedt, R. P.; Maurice, L. Q. *J. Propulsion Power* **2000**, *16*, 187.
(7) Violi, A.; Yan, S.; Eddings, E. G.; Sarofim, A. F.; Granata, S.; Faravelli, T.; Ranzi, E. *Combust. Sci. Technol.* **2002**, *174*, 399.
(8) Eddings, E. G.; Yan, S.; William, C.; Sarofim, A. F. *Combust. Sci. Technol.* **2005**, *177*, 1.

10.1021/ef049742u CCC: $30.25
Published on Web 06/28/2005

Table 1. Composition of JP-8 and Surrogate (in wt %)[a]

Hex-12		JP-8	
n-C_8	2.25	*n*-paraffin	~ 28
n-C_{12}	33.59	branched paraffin	~29
n-C_{16}	17.85		
xylenes	10.47	monoaromatics	~18
tetralin	11.30	diaromatics	~2
Decalin	24.54	cycloparaffin	~20
		not determined	~3
sum	100.00		100

[a] The composition of JP-8 is done with GC/GC-MS in this laboratory.

Table 2. Some Properties of the JP-8 and Surrogate Fuels

properties	JP-8	Hex-12	Decalin	*i*-C_8/toluene
smoke point, mm	24.5	23.1	23.7	22.7
MW, g/mol	173.5[a]	152.2	138.3	108.0
VABP,[b] °C	220.2	215.7	187.0	104.9
flash point, °C	40.9	41.3	58	−5.6
latent heat,[c] kJ/kg	254.6	281.8	305.8	332.4
combustion heat, MJ/kg	44.9	44.6	42.55	43.45

[a] MW of JP-8 is estimated by an API empirical equation. [b] VABP refers to volumetric average boiling point, which is the mean of 10, 30, 50, 70, and 90% recovery temperature as determined in ASTM D86. [c] Latent heat is estimated at VABP.

as the oxidizer while feeding a monodisperse stream of fuel droplets generated by fuel pressurization (34.46 kPa) through an orifice disk (d = 50 mm). The flame was quenched in a water-cooled collection probe. Helium (25 L/min) was transpired through probe walls and was used to cool and transport the products of reaction through a Teflon filter (d = 0.2mm), where the soot aerosol was collected.

Soot Extraction. Soot/aerosol samples were extracted in a Soxhlet extraction apparatus with dichloromethane (DCM) for 24 h. Excess solvent was removed, and the samples (extract and residue) were allowed to dry at room temperature. The extractable fraction of the condensed aerosol is defined as the soluble organic fraction (SOF). Samples labeled as residue are the insoluble portion of the aerosol.

Samples were prepared for ^{13}C NMR analysis by dissolving the tar-like SOF in CD_2Cl_2 at ca. 2:3 v/v. Because of the richness of the data obtained, only the ^{13}C NMR results will be considered in this paper. Tetramethylsilane (TMS) was added (~1% vol) as an internal reference. All spectra were obtained at room temperature on a Varian Inova 500 MHz NMR spectrometer, operating at 499.62 MHz for protons and 125.64 MHz for carbon. The carbon spectra were acquired using an acquisition time of 3.0 s, a sweep width of 33.2 kHz, a pulse flip angle of 80° (5.1 ms), and a 30.0 s recycle delay. The spin lattice relaxation time (T_1) in the fuel is approximately 20 s and is reduced to approximately 7.0 s in the SOF. Solum et al. reported that the presence of static free radicals in the extracts can effectively shorten T_1.[10] Reversed-gated proton decoupling was used to suppress nuclear Overhauser effects (NOE). These experimental conditions will produce quantitative data. The spectra, resulting from 1500 scans and 5 Hz line broadening, were referenced to TMS at 0 ppm. Carbon aromaticity (f_a) is defined as the ratio of the intensity of all lines in the aromatic region (according to the assignment of chemical shifts) to the intensity of all lines in the aromatic plus aliphatic regions.

GC and GC−MS. The GC analysis was performed on Hewlett-Packard 5890 gas chromatographs equipped with a mass selective detector (HP 5971) and a flame-ionization detector. Initial fuel analysis was performed on a nonpolar Restek column (30 m × 0.25 mm × 0.25 μm; Rtx-1), injected at 308 K, and held for 2 min, with a 4 K/min ramp to 583 K. SOFs were analyzed with a 5 μL sample injected onto an HP-5 capillary column (30 m × 0.25 mm × 0.1 μm). The column temperature was programmed to hold at 313 K for the first 3 min, followed by a ramp at 4 K/min to 573 K, where it was held for 15 min prior to cooling. Chromatogram peaks were identified by molecular weight and by matching their retention times to those of reference standards. Species are quantified using area/concentration curves measured for those reference standards. The methods used are similar to that of Ledesman et al.[11]

Electron Spin Resonance (ESR) of Soot Residues. The measurements of the unpaired electron spin concentrations were carried out on a Bruker EMX ESR X-band spectrometer with an operating frequency of 9.75 GHz. A standard free radical (DPPH, available from Aldrich) was used to calibrate the measurement of free radical concentrations. All samples studied were treated under vacuum at 100 mTorr for 48 h and vacuum-sealed to exclude the effects of absorbed oxygen on the ESR spectra. The experiments were carried out at room temperature. Details on the preparation and measurements of graphite factors of soot samples follow the procedure reported by Jiang et al.[12]

Results and Discussion

Study of SOF of Soot Aerosols. The GC chromatogram of the uncombusted JP-8 sample used in this study is shown in Figure 1. More than 200 hydrocarbons can be identified. Three major hydrocarbon classes exist in JP-8: paraffins, cycloparaffins, and aromatics as shown in Table 1. Alkanes ranging from *n*-heptane to *n*-octadecane are found. In addition, approximately 70 aromatic compounds have been identified in JP-8, but no aromatic species larger than the isomers of tri-methylnaphthalene have been found. This formulation of aromatic compounds satisfies the requirements of two related jet fuel regulations: the final distillation point is less than 573 K, and the smoke point is greater than 18 mm. Cycloparaffins from methylcyclopentane to *n*-decylcyclohexane as well as Decalin constitute the cycloparaffin structures present in the fuel. By performing a detailed hydrocarbon analysis with GC/GC−MS, the top three components in the JP-8 fuel are *n*-decane, *n*-undecane, and *n*-dodecane at 4.43, 4.43, and 3.63% (all in wt %), respectively.

Figure 2 shows the GC chromatograms corresponding to the SOFs of JP-8, Decalin, and Hex-12, all produced at 973 K. The chromatograms have been normalized by total peak area, so that relative yields of individual compounds can be seen. In general, the spectra from all three fuels are very similar. However, two features in particular are noteworthy. First, the chromatogram of Hex-12 has a much larger peak at 29 min than the other two fuels. This peak is identified as *n*-hexadecane, the heaviest component of the Hex-12 surrogate. Because there is no particular reason for the surrogate alone to form large amounts of cetane, we interpret this peak to be residual fuel. In the Decalin SOF chromatogram, there are no peaks corresponding to residual fuel, while in the JP-8 chromatogram, some of the peaks that

(9) Hanson, S. P. The Evolution of Fuel Nitrogen During the Vaporization of Heavy Fuel Oil Droplet Arrays. Ph.D. Thesis, Massachusetts Institute of Technology, 1982.
(10) Solum, M. S.; Veranth, J. M.; Jiang, Y. J.; Orendt, A. M.; Sarofim, A. F.; Pugmire, R. J. *Energy Fuels* **2003**, *17*, 738.
(11) Ledesma, E. B.; Marsh, N. D.; Sandrowitz, A. K.; Wornat, M. J. *Energy Fuels* **2002**, *16*, 1331.
(12) Jiang, Y. J.; Solum, M. S.; Pugmire, R. J.; Grant, D. M. *Energy Fuels* **2002**, *16*, 1296.

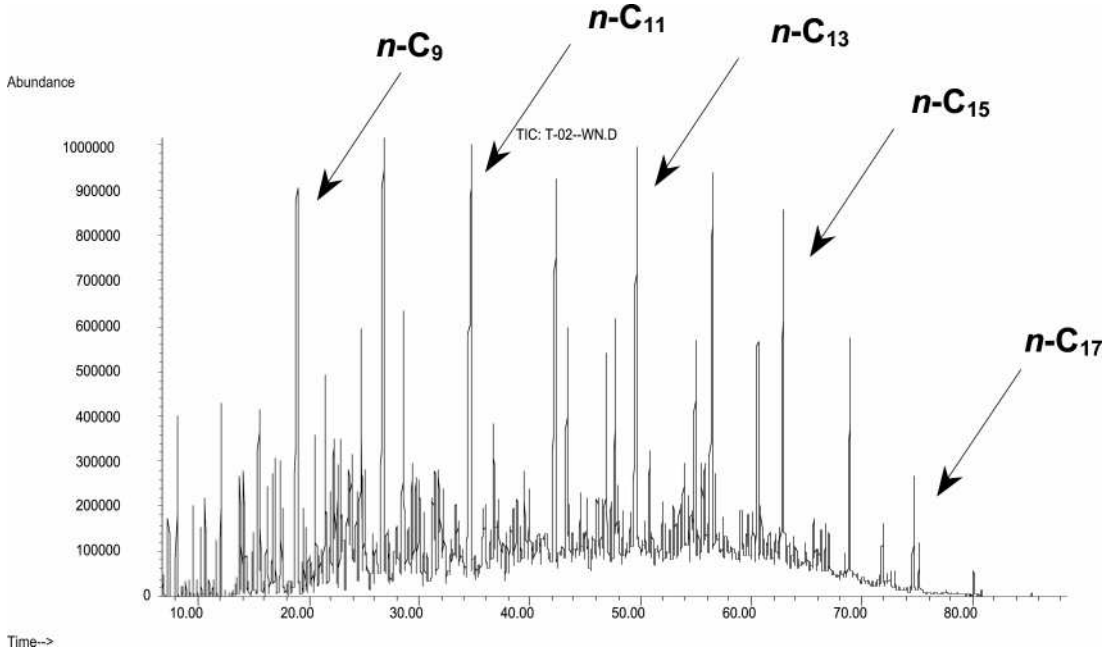

Figure 1. GC chromatogram of uncombusted JP-8.

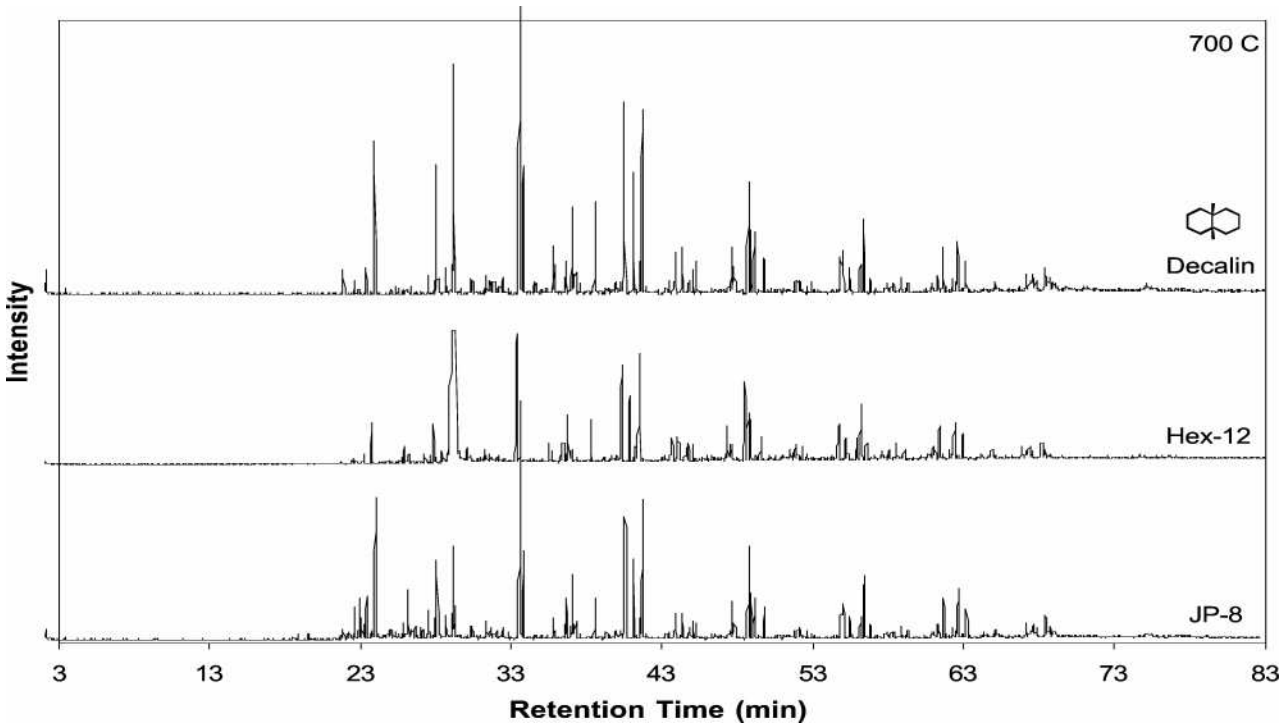

Figure 2. GC chromatogram of SOFs from JP-8, Hex-12, and Decalin soot aerosols created at 973 K furnace wall temperature.

appear before 29 min may represent unburned fuel rather than combustion products.

The other apparent difference between the chromatograms in Figure 2 lies in the three peaks between 40 and 42 min. These three peaks are identified as the isomers of molecular weight 202: fluoranthene, acephenanthrylene, and pyrene. It is evident in the chromatograms, and also from the calibrated yields based on peak areas, that the relative yields of these three isomers are quite similar between JP-8 and Hex-12 but are different for Decalin. Further evidence is obtained from additional soot aerosols that were generated and analyzed by GC at higher furnace temperatures (1073 and 1173 K). In fact, across three reactor temperatures, the following trend holds: for JP-8 and Hex-12 SOFs, pyrene is produced in greater yields than fluoranthene. However, at all three temperatures, in the Decalin SOFs, fluoranthene is the most prevalent isomer. It is clear that in terms of bulk properties such as aromatic fraction, Decalin can accurately model JP-8 under these test conditions. In terms of detailed chemistry, however, Decalin produces relative yields that are less representative of JP-8 than the Hex-12 surrogate.

The ^{13}C NMR spectra of uncombusted JP-8 and Hex-12 are presented in Figure 3. In the aliphatic region, the presence of straight-chain alkanes is verified by the resonance lines at 14.2 ppm (α-CH_3), 22.9 ppm (β-CH_2), 29.7 ppm (γ-CH_2), 30.0 ppm (δ-CH_2), and 32.2 ppm (ϵ-

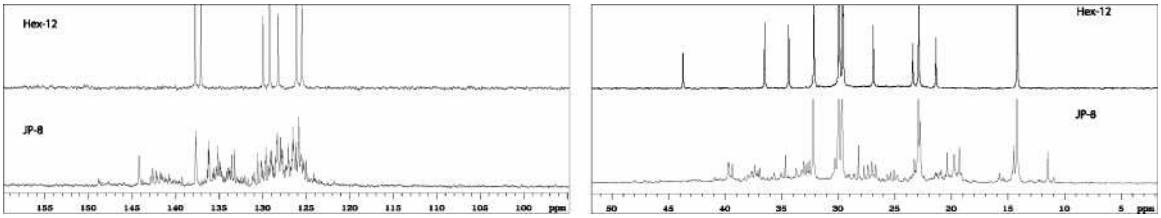

Figure 3. ^{13}C NMR spectrum of uncombusted JP-8 and Hex-12 at 125 MHz (left, aromatic region and right, aliphatic region).

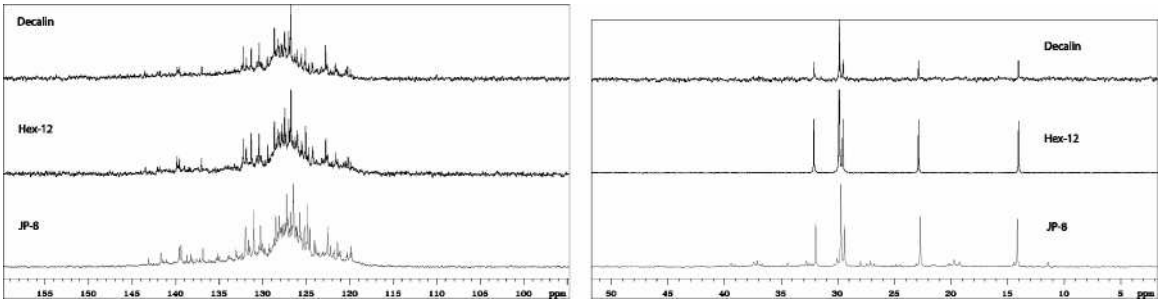

Figure 4. ^{13}C NMR spectrum of SOFs from JP-8, Hex-12, and Decalin soot aerosols at 125 MHz created at 973 K furnace wall temperature (left, aromatic region and right, aliphatic region).

CH_2), which corresponds to an *n*-alkane structure of $(\alpha\text{-}CH_3)_2(\beta\text{-}CH_2)_2(\gamma\text{-}CH_2)_2(\delta\text{-}CH_2)_2(\epsilon\text{-}CH_2)_y$, where the label e refers to CH_2 groups at the ϵ-position (and beyond) relative to the end methyl group (e.g., the central CH_2 group in *n*-nonane). Cookson and Smith[13] earlier suggested that the average *n*-alkane chain length, N_C, can be calculated from the formula

$$N_C = 8\frac{I(\alpha,\beta,\gamma,\delta,\epsilon)}{I(\alpha,\beta,\gamma,\delta)} \quad (1)$$

where *I* is the total ^{13}C NMR intensity due to the groups in parentheses. Using the integrated area for each peak, the average *n*-alkane chain length in the JP-8 is approximately 10.5. (For the purpose of comparison, the average *n*-alkane chain length calculated from eq 1 for the spectrum of 99.7% *n*-dodecane is 12.1.)

In the spectral region above 100 ppm, one can identify three general groups of resonance lines at approximately: 120 to ~128 ppm, 128 to ~135 ppm, and 135 to ~145 ppm, which roughly corresponds to protonated carbons in aromatics, condensed ring aromatics including bridgehead carbons (e.g., nonprotonated aromatic carbons that are common to two or more condensed aromatic rings), and alkyl- or aryl-substituted aromatics. Since no detectable lines are observed in the region from 100 to ~120 ppm from the spectrum of JP-8, one can conclude that the content of olefinic structures, including the indene type compounds, is too low to detect under these analytical conditions. Other hydroaromatic compounds, such as tetralin and indan, may exist. Also, three ring structures such as perhydrofluorene may exist. No resonance lines are found beyond 150 ppm, suggesting that the content of oxygenated aromatic compounds in JP-8 is under the detection limit as well. In addition to the compounds mentioned previously, the assignment of chemical shifts of other structural types in ^{13}C spectra are summarized in ref 14. These assignments are comparable to previous studies and based on model compound measurements.[13,15]

The ^{13}C NMR spectra of the SOF from JP-8, Hex-12, and Decalin aerosols generated at 973 K (furnace wall temperature) are presented in Figure 4. In the aliphatic region, there are two interesting features. First, the aliphatic portion of the SOF of JP-8 has been greatly simplified when compared with those of the uncombusted fuel (see Figure 3) (e.g., a disproportionate decrease in the intensity of the aliphatic structures not belonging to the *n*-alkane series is noted). While a wide variety of aliphatic structures is still present, the relative amounts of these structures have significantly changed vis a vis the normal alkanes. The aliphatic regions of the spectra of Hex-12 and Decalin SOFs exhibit similar features. Second, the average chain length of *n*-alkanes in the SOF of JP-8, Hex-12, and Decalin are 16.4, 15.3, and 17.4, respectively. Hence, relatively large amounts of 15−17 carbon *n*-alkanes exist in the SOF samples. For Hex-12, this amount may be as large as 45% of the SOF. The GC data (see Figure 2) also indicate that *n*-hexadecane is the predominant component. It is reasonable to assume that the *n*-alkanes in the SOF of Hex-12 and JP-8 are remnants of the unburned original fuel due to their low volatility. But for Decalin, the 4.5% *n*-C_{17} or C_{18} can only be generated during the combustion process by radical addition to an existing large aliphatic structure, which is an interesting alternative to that of aromatic ring formation and condensation. To confirm this unusual observation, the SOFs of *n*-dodecane and *i*-C_8/toluene (generated at furnace wall temperature 973 K) were also examined. Within the detection limits, no other resonance lines are observed in the aliphatic region except those arising for straight chain alkanes. The average chain lengths are 14 and 17 in these SOF fractions in which the total aliphatic carbon content of the two samples is 2 and 22% (in mol %), respectively. The formation of straight chain alkanes from Decalin (a cyclic paraffin consisting of two rings fused in either a

(13) Cookson, D. J.; Smith, B. E. *Anal. Chem.* **1985**, *57*, 864.
(14) Japanwala, S.; Chung, K. H.; Dettman, H. D.; Gray, M. R. *Energy Fuels* **2002**, *16*, 477.
(15) Snape, C. E.; Lander, W. R. *Anal. Chem.* **1979**, *51*, 2189.

Table 3. Properties of Soot Aerosols from Various Fuels[a]

fuel	I.P. (cm)	soot yield (wt %)	SOF yield (wt %)	f_a (mol %)	GF (%)	S.C. (10^{19})	LW (G)
JP-8	10.5	8.2	30.0	73.9	44.10	4.53	2.49
Hex-12	11.5	8.9	19.5	55.4	34.10	2.56	5.10
Decalin	9.0	8.9	13.2	95.5	72.37	1.93	5.47
i-C_8/toluene	5.5	8.8	8.3	78.3	53.55	3.60	3.43
n-C_{12}	13.0	4.5	42.0	98.0	72.51	1.38	8.17

[a] I.P., ignition point; G.F., graphite factor; S.C., spin concentration of unpaired electrons in the soot residue; and L.W., the line width of the ESR resonance line of the soot residue in gauss.

Table 4. PAH Compounds Identified in SOF from JP-8 at 973 K Furnace Temperature[a]

compound	yield (mg/mg)
acenaphthylene	23.5
acenaphthene	0.9
fluorine	10.1
phenanthrene	33.1
anthracene	10.2
flouranthene	17.5
acephenanthrylene	9.6
acenanthralene	3.0
pyrene	23.6

[a] These PAHs were also found in the Hex-12 and Decalin SOF.

cis or a trans configuration) SOF might suggest that ring opening and alkane formation is a parallel but less significant route in the evolution from fuel to soot. Comparable data have not previously been observed.

In the aromatic chemical shift region (beyond 100 ppm), resonance lines are found in the 120−145 ppm region of all SOFs. In PAH structures, the chemical shift region for both protonated and bridgehead carbons overlap considerably and are mostly restricted to ~122−135 ppm. Spectral lines in excess of 135 ppm arise primarily from alkyl (or oxygen) substituted aromatic compounds or from aryl−aryl linkages that arise in polymerization reactions that have been shown to be major contributors in the early evolution of aerosols made from anthracene,[10,16,17] phenanthrene,[16] pyrene, and biphenyl.[18,19] The extremes of this chemical shift range also suggest the formation of a host of aromatic structures containing five member rings such as indan, acenaphthene, fluorene, fluoranthane, ^{11}H-benzo[*a*]fluorene, indene, and acenaphthylene, etc. Evidence from GC/MS data for the formation of these types of aromatic structures has been identified in the SOFs produced from JP-8, Hex-12, and Decalin (see Table 4). The chemical shifts arising from the larger aromatic ring structures (anthracene, phenanthrene, pyrene, etc.) are buried within hundreds of overlapping resonance lines in the 124−134 ppm range and, thus, are not readily identifiable by simple NMR techniques. There seems to be an apparent discrepancy among the data listed in Tables 3and 4. The SOF of JP-8 soot in Table 3 exhibits a carbon aromaticity of 73.9% (mol %). Ironically, the sum of identified PAH compounds from this sample listed in Table 4 is at most 13% (wt %). The explanation of this apparent discrepancy is straightforward. In GC/GC−MS data, only the most abundant PAH species can be identified. In the NMR data, it is easy to quantify the sum of all PAH species as they share the same chemical shift region, whereas to identify a specific compound is more challenging with simple NMR techniques from such complex mixtures. This paradoxical result actually reflects the difficulty in the study of complex mixtures such as SOF of soot and justifies the use of multiple analytical techniques in this work with both SOF and residues that are discussed below.

The extent of PAH ring substitution could be estimated from the NMR data as well. The definition of aromaticity f_a in these samples is mentioned in the Experimental Procedures, and the data are given in Table 3. To illustrate this idea, we use the SOF of *n*-decalin as an example. In this sample, the aromaticity is 95.5%. A closer investigation of Figure 4 indicates that about 15.5% of the aromatic carbons is found in the chemical shift range attributed to substituted aromatic structures (~135−145 ppm). As discussed earlier, these resonance lines in this region might correspond to two types of structures: alkyl- or aryl-substituted aromatics. Even if all the aliphatic carbons in this sample are attached to the aromatic rings that will form alkyl-substituted aromatics, the biaryl linkage is still as high as 11%. While it is true that some of the carbon atoms in this chemical shift region can be attributed to the presence of five-membered rings fused to six-membered structures, the GC/MS data do not indicate that the abundance of structures of this type is sufficient to account for all of the carbons observed in this spectral window. Furthermore, the NMR data provide no evidence that a significant portion of the alkane structures is connected to an aromatic ring. Hence, under these experimental conditions, the data indicate the presence of biaryl linkages that may include as much as 12% of the total aromatic carbons. Previous work in this laboratory has identified substantial amounts of biaryl linkages in SOFs obtained from pyrolysis of biphenyl, pyrene, and phenanthrene (2−10% of the phenanthrene carbon atoms in the samples generated in a drop tube furnace at temperatures of 1300, 1400, and 1450 K).[20]

In the study of SOFs from all samples, oxygen functional groups have not been observed at a significant concentration level by either NMR or GC−MS. This is quite different from an early study on the extracts of flame generated soots by Akhter et al.[21] The soot samples were generated from a *n*-hexane flame, although it is not clear whether a premixed or diffusion flame was used. Five different solvents, *n*-hexane, benzene, chloroform, tetrahydrofuran, and acetonitrile, were used to extract the soot collected in these experiments. On the basis of FT−IR data, the presence of

(16) Pugmire, R. J.; Jiang, Y. J.; Solum, M. S.; Sarofim, A. F.; Veranth, J. M.; Schobert, H. H.; Pappano, P. J. *ACS Fuel Chemistry, Preprints* **2002**, *47*, 733.
(17) Wornat, M. J.; Lafleur, A. L.; Sarofim, A. F. *Polycyclic Aromat. Compd.* **1993**, *3*, 149.
(18) Solum, M. S.; Sarofim, A. F.; Pugmire, R. J.; Fletcher, T. H.; Zhang, H.-F. *Energy Fuels* **2001**, *15*, 961.
(19) Tomczyk, N. A.; Winance, R. E.; Solum, M. S.; Pugmire, R. J.; Fletcher, T. H. *ACS Fuel Chemistry, Preprints* **2002**, *47*, 731.
(20) Yan, S.; Solum, M. S.; Pugmire, R. J. Unpublished results, 2003.
(21) Akhter, M. S.; Chughtai, A. R.; Smith, D. M. *Appl. Spectrosc.* **1985**, *39*, 154.

carbonyl and C−O bonds as well as other oxygenated compounds was reported. Proton NMR data on these samples were also used to assign possible oxygen functional groups. Elemental analysis of their soot samples indicated oxygen contents ranging from 6 to 11%. However, in Akhter's study, only proton NMR data were obtained on the SOF. With oxygen contents at this level, corresponding resonance lines should be easily detected from ^{13}C NMR data. In our study, both proton and ^{13}C NMR are used to examine the SOF samples, and such oxygen functional groups are not observed. The differences may be due to combustion conditions.

As most SOF studies focus on soot/particulates formed in diesel engines, it is known that the properties of these particulates are affected by fuel properties.[22] Given the significant compositional differences among fuels tested in this study, it is plausible to assume that the soot aerosols formed from these fuels might have different properties even under similar test conditions. Some combustion related properties of these fuels have been included in this study, such as the ignition point of the fuel, the yield of soot aerosol, the yield of SOF, and the aromaticity of SOF, etc. The result is given in Table 3. The ignition point is defined as the distance from the point where droplets leave the orifice to the point where the flame is observed. The ignition point mainly reflects the average volatility of the fuel under the test conditions. The ignition point of surrogate Hex-12 is very close to that of JP-8, while the mixture of *i*-C_8/toluene has the shortest ignition point due to the low boiling point of its constituents. With the exception of *n*-dodecane, gross soot yields (Table 3) of these fuels are quite similar, which is in agreement with their similar smoke point values. Theoretically, the ignition point will determine the level of air premixing into the lifted diffusion flame, thereby facilitating soot oxidation. Among these fuels, even though the ignition point of *n*-dodecane is close to those of JP-8 and Hex-12, its soot yield is only half as much as the latter two fuels due to the presence of aromatic compounds in these fuels. The yield of SOF from soot samples examined varies between 8.3 and 42%. Kitamura reported that the soot residues in a diesel engine arise mainly from paraffinic hydrocarbons, whereas the source of SOF is mainly from aromatic hydrocarbons.[23] In our results, the paraffinic fuel *n*-dodecane provides a high yield of SOF (Table 3), even higher than the highly aromatic fuel JP-8. Hence, the production of SOF does not appear to be directly related to the type of fuel in question.

Study of Soot Residues. Solid state ^{13}C NMR has been successfully used in the past to study coal and soot structures.[10,18,24] However, some soot materials containing relatively large amounts of turbostratic structure (a mixture of amorphous carbon and large disordered PAH structures, sometimes referred to as graphenes) do not produce high quality NMR data due to sample conductivity. The conductivity is due to the high concentration of free electrons found in soot residues. Jiang et al.[12] developed a method for comparing the conductivity of aerosol residues by means of a simple measurement of the *Q*-value of an RF coil in which a sample has been placed. By comparing the *Q*-value of a soot sample with that of a set of standard graphite samples mixed with varying amounts of inert material, one can compare the conductivity of an unknown sample with a sample in which the amount of graphitic content is known. From these data, one can derive a graphite factor for the samples in question. This method then provides a means for estimating the relative amount of turbostratic structure present in a given soot sample. TEM data on soot residues studied reveal the presence of a disordered structure interspersed with areas where ordered structures are apparent.[25] However, to date we have not observed ordered structures with lattice spacing as small as that in graphite; hence, the term graphite factor refers to the relative amount of turbostratic structure in a carbon sample. The free radical concentrations in soot samples studied in the Utah laboratory can be as high as 10^{21} spins/g and are extremely stable when stored in a vacuum-sealed sample tube. The spin concentrations for the residues of this study are given in Table 3. The ESR line-widths range between 2.5 and 8.2 G. The Lande *g*-factors indicate that the electron environment is essentially the same in all samples (2.00258−2.00266) (e.g., carbon based radicals). The *g*-values for graphite are in the range of 2.005−2.015. The SOF material contains stable free radical concentrations that are ∼2 orders of magnitude lower than that of the residues. Hence, soot particles present an environmental and health risk that may not be totally appreciated.

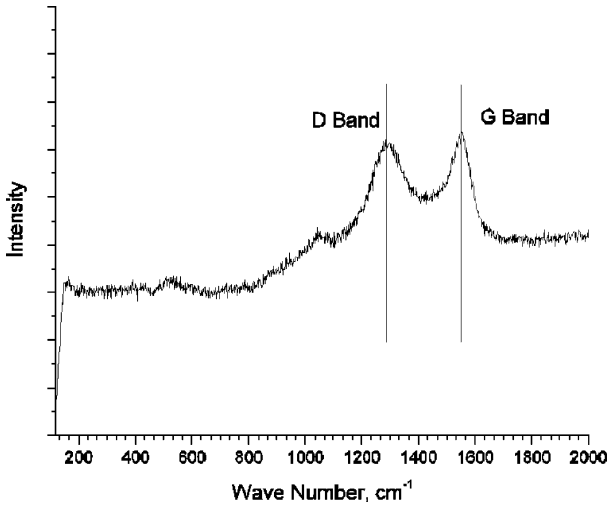

Figure 5. Raman spectrum of JP-8 soot residue created at 973 K furnace wall temperature (laser wavelength, 532 nm).

Raman spectroscopy, a common technique in graphite studies, was also utilized to examine these samples. The Raman spectrum of the JP-8 soot residue is shown in Figure 5.[26] A narrow G-band (∼1575 cm^{-1}) and a broader D-band (1200 to ∼1400 cm^{-1}) are observed. The G-band is derived from in-plane displacement in graphite and is the only band found in highly orientated pyrolytic graphite (HOPG) crystals. The D-band is disorder induced, and the ratio of the areas of the D- and G-band (I_D/I_G) is used as an indicator of the extent

(22) Tosaka, S.; Fujiwara, Y. *JSAE Rev.* **2000**, *21*, 463.
(23) Kitamura, T.; Ito, T.; Senda, J.; Fujimoto, H. *JSAE Rev.* **2001**, *22*, 139.
(24) Solum, M. S.; Pugmire, R. J.; Grant, D. M. *Energy Fuels* **1989**, *3*, 187.
(25) Pappano, P. J.; Schobert, H. H. *ACS Fuel Chemistry, Preprints* **1999**, *44*, 567.
(26) Pefferlle, L. Personal communication, 2003.

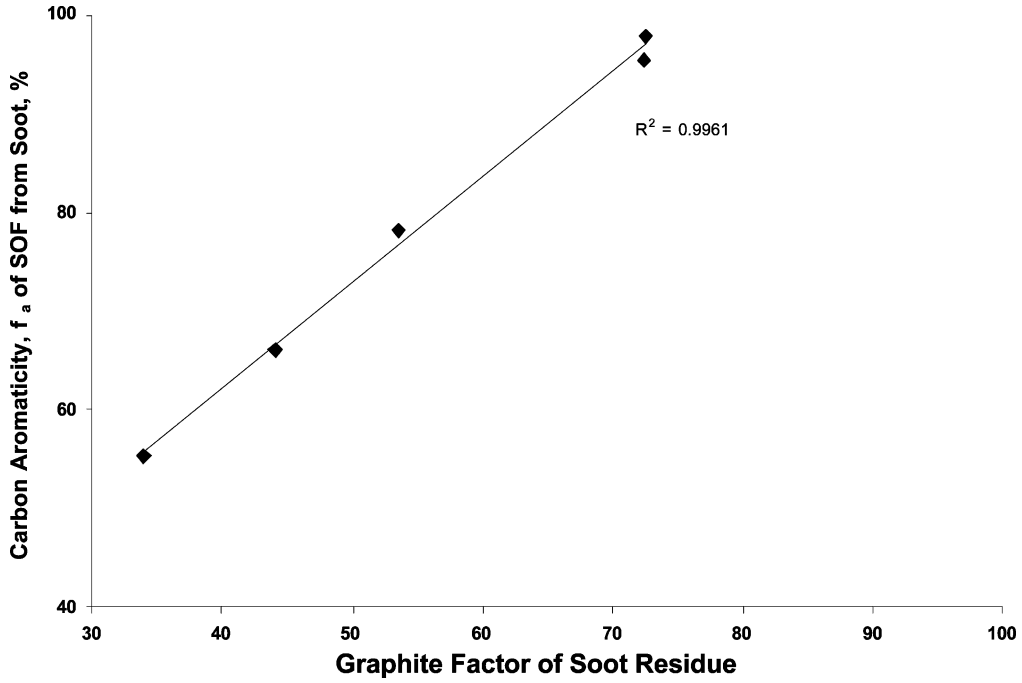

Figure 6. Correlation of SOF aromaticity with graphite factor/turbostratic structure of the soot residues from the five fuels studied.

of disorder or as a measure of the size of the graphitic sheets. Compared with a reference spectrum, the Raman spectrum of the JP-8 soot residue is similar to that of a highly disordered pre-graphitic material. This result is consistent with the Raman study of hexane soot by Akhter.[27] The D-band is further attributed to the aromatic skeleton vibrational modes of condensed aromatic rings. Raman spectra of other soot residues were also examined, but the results are identical to the JP-8 soot residue. Akhter also employed ESR to study the stable free radicals in the hexane soot.[27] The Lande g-value reported is 2.0058, and the line width is 3.25 G. While the line width is similar to those in Table 3, the *g*-value from Akhter's data (i.e., essentially that of graphite) is much larger than those found in this study.

An interesting linear correlation is noted between the carbon aromaticity of the SOFs and the graphite factors of the corresponding soot residues (see Figure 6). While it may be premature to reach a definitive conclusion, the data suggest that a strong correlation exists between the aromaticity of the SOF and the amount of turbostratic structure associated with the soot residues. It may be reasonable to assume that as the aromaticity (and size of the ring structures) of the SOF material increases, the transformation of the young soot (i.e., precarbonized material) to turbostratic material is facilitated. This relationship between aromaticity and the graphite factor seems to suggest that the SOF consists of a wide range of molecular structures that has not yet reached the point of incorporation into the soot structure. As the kinetics drive these reactions, the unincorporated tar appears to evolve in a manner parallel to the soot into larger, more aromatic structures prior to their incorporation into the insoluble residue, which continues to develop a higher degree of ordered/turbostratic structure. This observation needs further careful study.

Conclusion

Soot aerosols were generated in a drop-tube furnace with optical access from JP-8, a surrogate fuel, and other fuels. The soluble organic fractions (SOF) of soot aerosols were studied with GC, GC−MS, and ^{13}C NMR. The SOFs of these fuel aerosols consist primarily of PAH and small amounts of straight chain alkanes. The only variations are in the amount of straight chain alkanes and certain PAH isomers. Analysis on these SOFs indicates that Hex-12, a surrogate fuel, is capable of reproducing PAH profiles similar to those observed in JP-8 under these test conditions.

The insoluble portion of soot (residue) was studied with Raman spectroscopy, ESR, and graphite factor measurements. Raman studies on soot residues produced remarkably similar results; all residues are of highly disordered graphitic structures, while the other techniques used to examine the residues illustrated a significant variation in the ESR and conductivity behavior of these samples, suggesting that significant differences in structure exist. Soot residues produced under the same test conditions but from different fuels exhibited variations in their conductivity, apparent turbostratic structure, and ESR line-width. One can only conclude that the nature of the fuel plays a role in the evolution of the SOF and the residue as noted by the NMR data and the graphite factor measurements. Hence, in the experiments performed, the data demonstrate that the aerosols formed do not pass through a phase of complete structural degradation prior to the assembly of the fuel fragments into SOF and soot. Furthermore, the highly correlated aromaticity of the SOF with the graphite factor of the insoluble fraction of each individual fuel aerosol residue suggests that the SOF structural moieties have some relationship to the

(27) Akhter, M. S.; Chughtai, A. R.; Smith, D. M. *Appl. Spectrosc.* **1985**, *39*, 143.

initial structure of the aerosol residue. The study of the formation of these young soots in the early stages of soot formation should provide clues as to the formation mechanisms at relatively low temperatures.

Acknowledgment. The University of Utah gratefully acknowledges the support of the Department of Energy as part of the Advanced Strategic Computing Program through Contract B341493 from the Lawrence Livermore National Laboratory and the National Science Foundation CRAEMS Grant CHE0089133. Dr. Mark Solum is acknowledged for many helpful discussions regarding spectral assignments. Appreciation is extended to Prof. Lisa Pfefferle, who provided the Raman spectra of soot residues used in this study.

EF049742U